






## Analyzing the Performance of TAS/MRC with Decode-and-Forward Relaying for Multihop Transmission over Fisher-Snedecor $F$ Fading Channels

Hubha Saikia and Rajkishur Mudoi\*

Department of Electronics and Communication Engineering, North-Eastern Hill University,  
Shillong, Meghalaya, 793022, India



E-mail/Orcid Id:

HS,  [hubhasaikia9@gmail.com](mailto:hubhasaikia9@gmail.com); RM,  [rajkishur@gmail.com](mailto:rajkishur@gmail.com),  <https://orcid.org/0000-0003-3458-2419>

### Article History:

Received: 28<sup>th</sup> May, 2023

Accepted: 10<sup>th</sup> Dec., 2023

Published: 30<sup>th</sup> Dec., 2023

### Keywords:

ASER, Decode and Forward, Fisher-Snedecor  $F$  fading, MRC, Multihop, RQAM, TAS, XQAM

### How to cite this Article:

Hubha Saikia and Rajkishur Mudoi (2023). Analyzing the Performance of TAS/MRC with Decode-and-Forward Relaying for Multihop Transmission over Fisher-Snedecor  $F$  Fading Channels. *International Journal of Experimental Research and Review*, 36, 116-126.

### DOI:

<https://doi.org/10.52756/ijerr.2023.v36.011>

**Abstract:** This study comprehensively assesses a decode-and-forward relaying system that employs Transmit Antenna Selection/Maximal Ratio Combining (TAS/MRC) for multi-hop communication across Fisher-Snedecor  $F$  fading channels. The study primarily focuses on the average symbol error rate (ASER) and outage probability (OP) while using cross QAM (XQAM) and rectangular quadrature amplitude modulation (RQAM). The proposed MIMO system effectively decreases the hardware complexity and cost of large antennas by implementing Transmit Antenna Selection (TAS) at the source and relay nodes and Maximum Ratio Combining (MRC) diversity at the destination and relays. Analytical formulations for OP (outage probability) and ASER (average symbol error rate) are derived using PDF (Probability Density Function)-based methods. Monte-Carlo simulations further validate these formulas. The investigation indicates that system performance is improved under conditions of lighter shadowing compared to moderate and extreme shadowing settings. Additionally, increasing the hop count amplifies the observed performance. Moreover, when the fading parameter increases, both the OP and ASER decrease. This study comprehensively examines the impact of many parameters, including  $m$ ,  $p$ ,  $L$ ,  $R$ , and  $o$ , on the behaviour of the system under Fisher-Snedecor  $F$  fading. Based on the findings, the combination of shadowing and multipath fading significantly affects the system's performance, with both  $m$  and  $p$  significantly influencing this. When examining the Signal-to-Noise Ratio (SNR), a comparison between RQAM and XQAM demonstrates that XQAM is superior. The research uncovers crucial information for planning and executing the TAS/MRC-based MIMO multi-hop communication system. This technology possesses the capability to enhance the effectiveness of similar communication systems, as seen by the encouraging advancements in performance, especially in scenarios including signal attenuation.

### Introduction

MIMO system is one of the most modernized technologies that fulfil the high bit rate demand of wireless communication. The multipath fading dissipation in system communication is lowered by MIMO (Foschini and Gans, 1998). The MIMO system utilizes a vast number of antennas, causing an increase in the apparatus's intricacy and cost. The TAS equipped with MRC at the receiver is utilized to solve these problems. TAS/MRC reduces the complication of the system by a great deal. In the TAS scheme, the channel state information (CSI) is put back to the transmitter and based on CSI, the transmit antenna that maximizes the

SNR at the receiver output is chosen to send the signal (Molisch and Win, 2004; Kumbhani and Kshetrimayum, 2016). Cooperative communication is another effective technology where the coverage and reliability of a wireless broadcasting system can be increased. The effectiveness of the signal is enhanced with the help of an intervening terminal known as a relay, which redirects the information received to the required target when the passage between the source and the user is weak (Sendonaris et al., 2003; Laneman et al., 2004). The feature of MIMO can also be implemented in cooperative communication systems to improve the overall system performance (Nosratinia et al., 2004). The two varieties



of suitable relays are i) decode and forward relaying (DF), whereby the message signal is decoded and then it is re-encoded and forwarded to the destination, and ii) amplify and forward relaying (AF), where the received signal is amplified, and then it is delivered to the desired destination. In AF, relaying noise is also amplified. Recently, multihop relay communication has gained significant importance because of its profitable and favourable approach to expanding the network and removing the dull patches of a wireless network (Pabst et al., 2004; Oyman et al., 2007). In wireless implementation, the method of transferring digital data by employing analogue signals simultaneously and successfully implementing bandwidth of channels has gained exposure to quadrature amplitude modulation (QAM) techniques. QAM signals may be applied in high-speed mobile communication, microwaves, etc. In QAM schemes, on the basis of the channel requirement, the constellation size of the signals can also be adjusted. So, QAM methods have drawn immense attention from researchers (Stuber, 2003). There are various QAM schemes, viz. rectangular QAM (RQAM), cross QAM (XQAM), square QAM (SQAM), etc. RQAM overlays different familiar modulations viz. SQAM, binary phase-shift keying (BPSK), quadrature phase-shift keying, orthogonal BPSK, etc. (Proakis, 2001). Among the QAM mentioned above signalling, XQAM can be considered the excellent QAM signalling due to its ability to transmit the odd number of bits due to its low average symbol energy in contrast to RQAM (Zhang et al., 2010). The system's channel is considered to be experienced by Fisher-Snedecor  $F$  fading distribution. Fisher-Snedecor  $F$  fading has been suggested recently to model system communication operating in outside and inside environments at 5.8 GHz and gives better performance to the channels operating under non-line-of-sight (LOS) and LOS fading surroundings. Fisher-Snedecor  $F$  fading channel can also be utilized for some common fading channels like the Nakagami- $m$ , one-sided Gaussian distribution and Rayleigh fading channel (Yoo et al., 2017).

Few research works on the performance of outage probability (OP) and average symbol error rate (ASER) in wireless network functioning under different fading environments have been found in the literature. In (Molisch and Win, 2004; Sanayei and Nosratinia, 2004), the authors have simultaneously applied selection diversity to both the transmitter and receiver to conserve the advantages of the MIMO system and, at the same time, reduce the cost of utilizing multiple RF elements. The authors (Banu et al., 2022) have analyzed the ASER

performance using MRC schemes with moment generating function (MGF) for QAM modulation over uniformly distributed Rayleigh fading channel by employing DF dual-hop relaying. Another challenging task in cooperative communication is to select the best relay for setting up the transmission, so the authors in (Clarke and Lamare, 2012) proposed various relay selection and minimum power allotment algorithms. In (Ikki and Ahmed, 2010), the expressions for SER as well as asymptotic error probability have been presented for BPSK signals with the relay selection scheme under independent and non-identically distributed (i.n.i.d) Rayleigh fading channels for both adaptive DF and AF cooperative diversity. The multihop wireless network performance implying AF relaying over Rayleigh fading channels with the effect of cochannel interference has been studied (Ikki and Aissa, 2012).

Moreover, an approximate PDF expression of instantaneous SNR has been shown, and based on this, a closed-form expression has been derived for the error probability. The authors in (Bao and Kong, 2010) investigated the performance of multihop transmission over Rayleigh fading channel using DF relaying considering partial relay selection by implementing cluster-based multihop wireless networks that can improve the spectral efficiency and the power of transmission over direct transmission as well as conventional multi-hop transmission. In (Dixit and Sahu, 2013), the authors have presented the performance of ASER with RQAM as well as XQAM signals over two-wave diffuse power (TWDP) fading distribution. In (Shaik et al., 2019), the authors have analyzed the QAM techniques for MIMO based non-regenerative relaying communication subject to Nakagami- $m$  fading channel for maximizing the received signal power. RQAM has been executed in high-rate wireless, microwave, and telephonic line modems (Agarwal and Zeng, 2011; Rappaport, 2011). The authors (Smith, 1975) showed that XQAM gives optimum QAM signalling because of its less average symbol energy when the odd number of bits are transmitted compared to RQAM. For  $M$ -ary XQAM, the error probability expressions have been derived in using maximal ratio combining (MRC) under  $\eta$ - $\mu$  fading channel (Yu et al., 2011). In (Singya et al., 2018), the authors have shown the performance of HQAM and RQAM, implemented in an OFDM with 3-hop AF relaying and the execution over Rician/Rayleigh fading channels. The authors in (Badarneh et al., 2018) examined the performance of i.n.i.d Fisher-Snedecor  $F$  fading distribution applying MRC at the receiver. The authors analyzed the performance of receivers over i.n.i.d

Fisher-Snedecor  $F$  fading and used selection combining (Al-Hmood and Al-Raweshidy, 2021).

Previous works have obtained results for BER/SER, and OP utilizing various fading channels. However, the multihop TAS/MRC QAM signalling analysis over the Fisher-Snedecor  $F$  fading channel is hardly available. This motivated me to find the performance of the system's OP and the ASER performance for RQAM and XQAM signalling, respectively. The novelties of the article are-

- The overall PDF of the system is obtained with respect to the Gamma function.
- The OP of the transmission system is found.
- The ASER deploying RQAM and XQAM are analysed.

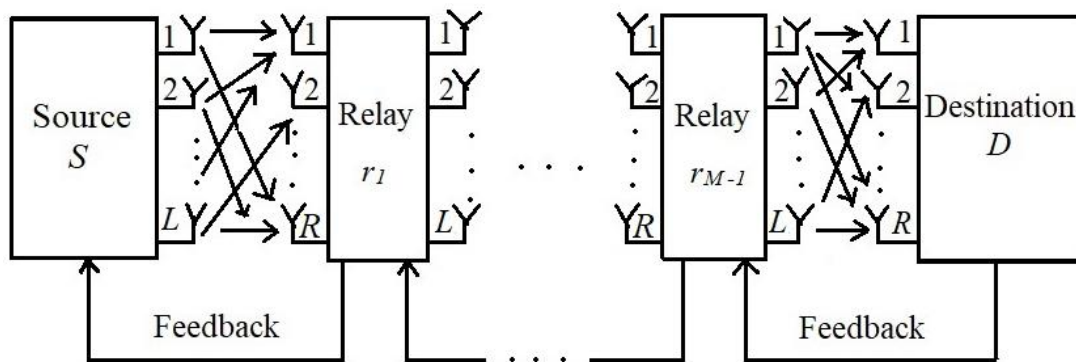


Figure 1. System Model.

**Materials and Methods**

A MIMO-based relaying communication is depicted in Figure 1 with  $M$  number of hops, a source  $S$ , a destination  $D$  and  $M-1$  DF relay nodes  $r_x$ , whereby  $x = \{1, 2, \dots, M-1\}$ . All the  $(M+1)$  nodes are sufficiently separated with equal distance. Therefore, a node can only receive signals from its adjacent nodes. Due to the long distance, there is no direct linkage between the source and the destination, and the information is transmitted from the source via  $M$  hops and  $M-1$  relays to the destination. The source and each relay are provided with  $L$  transmitting antennas. Similarly, each relay and destination are provided with  $R$ -receiving antennas. The receiving node of each hop sends the CSI to the transmitting node of that particular hop. Based on this CSI, the transmitter chooses the best transmit antenna, which maximizes the received SNR at that particular receiving node. On the receiving node, MRC is employed where the signals of all receiving antennas are added to maximize the output SNR. The channel of the system experiences Fisher-Snedecor  $F$  fading distribution. The fading coefficient of the  $w^{\text{th}}$  hop is represented by  $\alpha_w$  where  $w=1, 2, \dots, M$ . The transmitted power at  $w^{\text{th}}$  hop

is represented as  $\alpha_w$ , and the signal received at the node  $r_w$  from antenna  $j$  of node  $r_{w-1}$  (or at  $D$  from antenna  $j$  of  $r_{M-1}$ ) can be written as,

$$T_w^j = \sqrt{Z_w} \alpha_w \eta + \rho_w, \forall j \in [1, L], \dots \dots \dots (1)$$

where  $\eta$  is the complex base-band transmitted signal and  $\rho_w$  is the additive white Gaussian noise (AWGN) with variance  $N_0$ , that is, the one-sided power spectral.

If  $E_s$  denotes the average energy per symbol, the instantaneous SNR of the  $w^{\text{th}}$  hop can be defined as  $\gamma_w = |\alpha_w|^2 \frac{E_s}{N_0}$ . Considering the TAS/MRC system, the

CDF of the  $\gamma_w$  is derived from (Badarneh et al., 2018) as

$$F_{\gamma_w}(\gamma) = \left[ \frac{1}{\Gamma(1+mR)} \left( \frac{m}{p\gamma} \right)^{mR} \left\{ \frac{\Gamma(m+p)}{\Gamma(p)} \right\}^R \gamma^{mR} {}_2F_1 \left( m+p, mR; 1+mR, -\frac{m\gamma}{p\gamma} \right) \right]^L \dots \dots \dots (2)$$

Where  $m$  denotes the fading severity parameter,  $p$  is the shadowing parameter,  $\Gamma(\cdot)$  is the Gamma function, and  ${}_2F_1(\cdot)$  represents the Gauss hypergeometric function. The Gauss hypergeometric function in (2) can be expressed by infinite series representation using (Abramowitz and Stegun, 1970) as

$$F_{\gamma_w}(\gamma) = \frac{\{\Gamma(m+p)\}^{L(R-1)}}{\{\Gamma(mR)\}^L \{\Gamma(p)\}^{RL}} \left( \frac{m}{p\gamma} \right)^{mRL} \times \sum_{n_1=0}^{\infty} \sum_{n_2=0}^{\infty} \dots \sum_{n_L=0}^{\infty} \frac{\prod_{i=1}^L \{\Gamma(m+p+n_i)\Gamma(mR+n_i)\}}{\prod_{i=1}^L \{\Gamma(1+mR+n_i)(n_i)!\}} \left( -\frac{m}{p\gamma} \right)^{\sum_{i=1}^L n_i} \times \gamma^{\left( \frac{mRL + \sum_{i=1}^L n_i}{p\gamma} \right)} \dots \dots \dots (3)$$

The PDF can be obtained by differentiating the CDF of (3) as

$$f_{\gamma_w}(\gamma) = \frac{\{\Gamma(m+p)\}^{L(R-1)}}{\{\Gamma(mR)\}^L \{\Gamma(p)\}^{RL}} \left( \frac{m}{p\gamma} \right)^{mRL} \sum_{n_1=0}^{\infty} \sum_{n_2=0}^{\infty} \dots \sum_{n_L=0}^{\infty} \frac{\prod_{i=1}^L \{\Gamma(m+p+n_i)\Gamma(mR+n_i)\}}{\prod_{i=1}^L \{\Gamma(1+mR+n_i)(n_i)!\}} \left( -\frac{m}{p\gamma} \right)^{\sum_{i=1}^L n_i}$$

$$\times \left( mRL + \sum_{i=1}^L n_i \right) \gamma^{\left( mRL + \sum_{i=1}^L n_i \right) - 1} \dots \dots \dots (4)$$

The fixed gain DF-type relay can forward an incorrectly decoded signal to the next hop, and the weakest hop influences the complete system outage. Hence the MIMO with TAS/MRC and DF relaying transmission can be modelled statistically as an equivalent single hop transmission, and the joint PDF of output SNR can be obtained using (Bao and Kong, 2010) as

$$f_\gamma(\gamma) = \sum_{w=1}^M f_{\gamma_w}(\gamma) \prod_{\substack{y=1 \\ y \neq w}}^M [1 - F_{\gamma_y}(\gamma)] \dots \dots \dots (5)$$

Putting the values of (3) and (4) in (5), the expression of (5) is interpreted as

$$f_\gamma(\gamma) = \Delta \gamma^{\left( mRL + \sum_{i=1}^L n_i \right) - 1} \left\{ 1 - \Theta \gamma^{\left( mRL + \sum_{i=1}^L n_i \right)} \right\} \dots \dots \dots (6)$$

Where,

$$\Delta = \sum_{w=1}^M \prod_{\substack{y=1 \\ y \neq w}}^M \frac{\{\Gamma(m+p)\}^{L(R-1)}}{\{\Gamma(mR)\}^L \{\Gamma(p)\}^{RL}} \left( \frac{m}{p\gamma} \right)^{mRL} \times \sum_{n_1=0}^{\infty} \sum_{n_2=0}^{\infty} \dots \sum_{n_L=0}^{\infty} \frac{\prod_{i=1}^L \{\Gamma(m+p+n_i)\Gamma(mR+n_i)\}}{\prod_{i=1}^L \{\Gamma(1+mR+n_i)(n_i)!\}} \left( -\frac{m}{p\gamma} \right)^{\sum_{i=1}^L n_i} \left( mRL + \sum_{i=1}^L n_i \right)$$

and

$$\Theta = \frac{\{\Gamma(m+p)\}^{L(R-1)}}{\{\Gamma(mR)\}^L \{\Gamma(p)\}^{RL}} \left( \frac{m}{p\gamma} \right)^{mRL}$$

$$\times \sum_{n_1=0}^{\infty} \sum_{n_2=0}^{\infty} \dots \sum_{n_L=0}^{\infty} \frac{\prod_{i=1}^L \{\Gamma(m+p+n_i)\Gamma(mR+n_i)\}}{\prod_{i=1}^L \{\Gamma(1+mR+n_i)(n_i)!\}} \left( -\frac{m}{p\gamma} \right)^{\sum_{i=1}^L n_i} \dots$$

A flowchart of the proposed methodology is illustrated in Figure 2.

**Outage probability analysis**

For a multihop system, the OP occurs when the SNR of at least one hop goes below the threshold value,  $\gamma_{th}$ . The OP expression can be defined by (Dixit and Sahu, 2018) as

$$P_{out} = 1 - \prod_{w=1}^M [1 - F_{\gamma_w}(\gamma_{th})] \dots \dots \dots (7)$$

The OP expression can be obtained by putting  $\gamma = \gamma_{th}$  in (2) and substituting the value of (2) in (7),

$$P_{out} = 1 - \prod_{w=1}^M \left[ 1 - \left( \frac{1}{\Gamma(1+mR)} \left( \frac{m}{p\gamma} \right)^{mR} \left\{ \frac{\Gamma(m+p)}{\Gamma(p)} \right\}^R \gamma_{th}^{mR} {}_2F_1 \left( m+p, mR; 1+mR; -\frac{m\gamma_{th}}{p\gamma} \right) \right)^L \right] \dots \dots \dots (8)$$

**ASER analysis for RQAM**

The ASER considering the probability density function can be given as (Proakis, 2001)

$$p(e) = \int_0^{\infty} f_\gamma(\gamma) p(e|\gamma) d\gamma \dots \dots \dots (9)$$

Whereby  $p(e|\gamma)$  is the conditional error probability (CEP) and  $f_\gamma(\gamma)$  is the PDF of the system output SNR. A Y-ary RQAM signal constellation is created by using two separate quadrature Y-ary PAM signals. The in-phase signal is  $Y_I$ -ary PAM, whereas the quadrature signal is  $Y_Q$ -ary PAM. The Y-ary RQAM results in the yield of the CEP (Beaulieu, 2006).

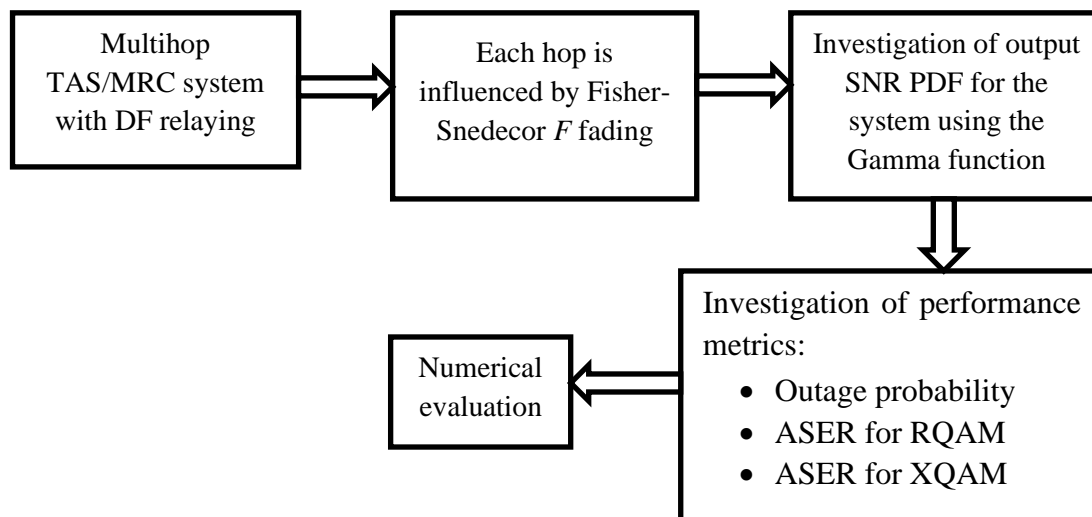


Figure 2. Flowchart of the proposed methodology.



$$p(e|\gamma) = 2\psi Q(a\sqrt{\gamma}) + 2\tau Q(b\sqrt{\gamma}) - 4\psi\tau Q(a\sqrt{\gamma})Q(b\sqrt{\gamma}) \dots\dots\dots(10)$$

Whereby, the Gaussian  $Q$ -function is denoted by  $Q(\cdot)$ ,

$$Y = Y_I \times Y_Q \quad , \quad \psi = 1 - \left(\frac{1}{Y_I}\right) \quad , \quad \tau = 1 - \left(\frac{1}{Y_Q}\right) \quad ,$$

$$a = \sqrt{\frac{6}{(Y_I^2 - 1) + (Y_Q^2 - 1)\beta^2}} \quad , \quad b = \beta a \quad \text{and} \quad \beta = \frac{d_Q}{d_I} \quad .$$

Here  $\beta$  is the quadrature to in-phase decision distance ratio;  $d_I$  and  $d_Q$  are the in-phase and quadrature decision distance, respectively.

Using  $Q(\theta) = \frac{1}{2} \operatorname{erfc}\left(\frac{\theta}{\sqrt{2}}\right)$  in (10), the expression consists of bivariate Meijer's  $G$  function, which is difficult to compute. So, Chiani approximation can be applied for  $Q(\cdot)$  and written as  $Q(\theta) \approx \frac{1}{12} e^{-\frac{\theta^2}{2}} + \frac{1}{4} e^{-\frac{2\theta^2}{3}}$  (Chiani et al., 2003). Putting Chiani approximation in (10),  $p(e|\gamma)$  can be expressed as

$$p(e|\gamma) = 2\psi \left( \frac{1}{12} e^{-\frac{(a\sqrt{\gamma})^2}{2}} + \frac{1}{4} e^{-\frac{2(a\sqrt{\gamma})^2}{3}} \right) + 2\tau \left( \frac{1}{12} e^{-\frac{(b\sqrt{\gamma})^2}{2}} + \frac{1}{4} e^{-\frac{2(b\sqrt{\gamma})^2}{3}} \right) - 4\psi\tau \left( \frac{1}{12} e^{-\frac{(a\sqrt{\gamma})^2}{2}} + \frac{1}{4} e^{-\frac{2(a\sqrt{\gamma})^2}{3}} \right) \left( \frac{1}{12} e^{-\frac{(b\sqrt{\gamma})^2}{2}} + \frac{1}{4} e^{-\frac{2(b\sqrt{\gamma})^2}{3}} \right) \dots\dots\dots(11)$$

Putting (6) and (11) in (9), the ASER can be written as

$$p(e)_{\text{ROAM}} = A_1 + A_2 - A_3 \dots\dots\dots(12)$$

where,

$$A_1 = 2\psi\Delta \int_0^\infty \gamma^{(mRL + \sum_{i=1}^L n_i) - 1} \left( \frac{1}{12} e^{-\frac{a^2}{2}\gamma} + \frac{1}{4} e^{-\frac{2a^2}{3}\gamma} \right) d\gamma - \Theta \int_0^\infty \gamma^{(2mRL + 2\sum_{i=1}^L n_i) - 1} \left( \frac{1}{12} e^{-\frac{a^2}{2}\gamma} + \frac{1}{4} e^{-\frac{2a^2}{3}\gamma} \right) d\gamma \dots\dots\dots(13)$$

$$A_2 = 2\tau\Delta \int_0^\infty \gamma^{(mRL + \sum_{i=1}^L n_i) - 1} \left( \frac{1}{12} e^{-\frac{b^2}{2}\gamma} + \frac{1}{4} e^{-\frac{2b^2}{3}\gamma} \right) d\gamma - \Theta \int_0^\infty \gamma^{(2mRL + 2\sum_{i=1}^L n_i) - 1} \left( \frac{1}{12} e^{-\frac{b^2}{2}\gamma} + \frac{1}{4} e^{-\frac{2b^2}{3}\gamma} \right) d\gamma \dots\dots\dots(14)$$

and,

$$A_3 = 4\psi\tau\Delta \left( \int_0^\infty \gamma^{(mRL + \sum_{i=1}^L n_i) - 1} \left( \frac{1}{144} e^{-\frac{(a^2+b^2)}{2}\gamma} + \frac{1}{48} e^{-\frac{(a^2+2b^2)}{3}\gamma} + \frac{1}{48} e^{-\frac{(2a^2+b^2)}{3}\gamma} + \frac{1}{16} e^{-\frac{(2a^2+2b^2)}{3}\gamma} \right) d\gamma - \Theta \int_0^\infty \gamma^{(2mRL + 2\sum_{i=1}^L n_i) - 1} \left( \frac{1}{144} e^{-\frac{(a^2+b^2)}{2}\gamma} + \frac{1}{48} e^{-\frac{(a^2+2b^2)}{3}\gamma} + \frac{1}{48} e^{-\frac{(2a^2+b^2)}{3}\gamma} + \frac{1}{16} e^{-\frac{(2a^2+2b^2)}{3}\gamma} \right) d\gamma \right) \dots\dots\dots(15)$$

Using (Gradshteyn and Ryzhik, 2000) to solve the integrals in (13), (14) and (15), the expressions can be written as,

$$A_1 = 2\psi\Delta \left( \left(\frac{\Upsilon}{12}\right) \left(\frac{a^2}{2}\right)^{-\left(mRL + \sum_{i=1}^L n_i\right)} + \left(\frac{\Upsilon}{4}\right) \left(\frac{2a^2}{3}\right)^{-\left(mRL + \sum_{i=1}^L n_i\right)} - \Theta \left\{ \left(\frac{\Omega}{12}\right) \left(\frac{a^2}{2}\right)^{-2\left(mRL + \sum_{i=1}^L n_i\right)} + \left(\frac{\Omega}{4}\right) \left(\frac{2a^2}{3}\right)^{-2\left(mRL + \sum_{i=1}^L n_i\right)} \right\} \right) \dots\dots\dots(16)$$

$$A_2 = 2\tau\Delta \left( \left(\frac{\Upsilon}{12}\right) \left(\frac{b^2}{2}\right)^{-\left(mRL + \sum_{i=1}^L n_i\right)} + \left(\frac{\Upsilon}{4}\right) \left(\frac{2b^2}{3}\right)^{-\left(mRL + \sum_{i=1}^L n_i\right)} - \Theta \left\{ \left(\frac{\Omega}{12}\right) \left(\frac{b^2}{2}\right)^{-2\left(mRL + \sum_{i=1}^L n_i\right)} + \left(\frac{\Omega}{4}\right) \left(\frac{2b^2}{3}\right)^{-2\left(mRL + \sum_{i=1}^L n_i\right)} \right\} \right) \dots\dots\dots(17)$$

and

$$A_3 = 4\psi\tau\Delta \left( \left(\frac{\Upsilon}{144}\right) \left(\frac{a^2+b^2}{2}\right)^{-\left(mRL + \sum_{i=1}^L n_i\right)} + \left(\frac{\Upsilon}{48}\right) \left(\frac{a^2+2b^2}{3}\right)^{-\left(mRL + \sum_{i=1}^L n_i\right)} + \left(\frac{\Upsilon}{48}\right) \left(\frac{2a^2+b^2}{3}\right)^{-\left(mRL + \sum_{i=1}^L n_i\right)} + \left(\frac{\Upsilon}{16}\right) \left(\frac{2a^2+2b^2}{3}\right)^{-\left(mRL + \sum_{i=1}^L n_i\right)} - \Theta \left\{ \left(\frac{\Omega}{144}\right) \left(\frac{a^2+b^2}{2}\right)^{-2\left(mRL + \sum_{i=1}^L n_i\right)} + \left(\frac{\Omega}{48}\right) \left(\frac{a^2+2b^2}{3}\right)^{-2\left(mRL + \sum_{i=1}^L n_i\right)} + \left(\frac{\Omega}{48}\right) \left(\frac{2a^2+b^2}{3}\right)^{-2\left(mRL + \sum_{i=1}^L n_i\right)} + \left(\frac{\Omega}{16}\right) \left(\frac{2a^2+2b^2}{3}\right)^{-2\left(mRL + \sum_{i=1}^L n_i\right)} \right\} \right) \dots\dots\dots(18)$$

Where,  $\Upsilon = \Gamma\left(mRL + \sum_{i=1}^L n_i\right)$  and  $\Omega = \Gamma\left(2mRL + 2\sum_{i=1}^L n_i\right)$ .

**ASER analysis for XQAM**

For XQAM,  $p(e|\gamma)$  is given as (Yu et al., 2011)

$$p(e|\gamma) = t_1 Q_c(g_0\sqrt{\gamma}, \pi/2) + \frac{4}{N} Q_c(g_1\sqrt{\gamma}, \pi/2) - t_2 Q_c(g_0\sqrt{\gamma}, \pi/4) - \frac{8}{N} \sum_{c=1}^{d-1} Q_c(g_0\sqrt{\gamma}, l_c) - \frac{4}{N} \sum_{c=1}^{d-1} Q_c(g_c\sqrt{\gamma}, s_c^+) + \frac{4}{N} \sum_{c=2}^d Q_c(g_c\sqrt{\gamma}, s_c^-) \dots\dots\dots(19)$$

whereby,  $N$  denotes the number of symbols and  $N = 2^5, 2^7, \dots$  ;  $d = \frac{\sqrt{2N}}{8}$  ;  $g_0 = \sqrt{\frac{96}{31N-32}}$  ;  $g_c = \sqrt{2c}g_0$  ,  $c = 1, 2, \dots, d$  ;  $t_1 = 4 - \frac{6}{\sqrt{2N}}$  ;

$$t_2 = 4 - \frac{12}{\sqrt{2N}} + \frac{12}{2N} \quad ; \quad l_c = \arctan\left(\frac{1}{2c+1}\right) ,$$

$$c = 1, 2, \dots, (d-1) \quad ; \quad s_k^+ = \arctan\left(\frac{c}{c+1}\right) ,$$

$$c = 1, 2, \dots, (d-1) \quad ; \quad s_k^- = \arctan\left(\frac{c}{c-1}\right), \quad c = 2, 3, \dots, d ;$$

$Q_z(\dots)$  is the generalized Marcum  $Q$ -function. Putting the value of (6) and (19) in (9),

$$p(e)_{XQAM} = \Delta \int_0^\infty \left[ t_1 Q_z(g_0 \sqrt{\gamma}, \pi/2) + \frac{4}{N} Q_z(g_1 \sqrt{\gamma}, \pi/2) - t_2 Q_z(g_0 \sqrt{\gamma}, \pi/4) - \frac{8}{N} \sum_{c=1}^{d-1} Q_z(g_0 \sqrt{\gamma}, l_c) \right. \\ \left. - \frac{4}{N} \sum_{c=1}^{d-1} Q_z(g_c \sqrt{\gamma}, s_c^+) + \frac{4}{N} \sum_{c=2}^d Q_z(g_c \sqrt{\gamma}, s_c^-) \right] \left\{ \gamma^{\left(mRL + \sum_{i=1}^L n_i\right)^{-1}} - \Theta \gamma^{\left(2mRL + 2 \sum_{i=1}^L n_i\right)^{-1}} \right\} d\gamma . \quad (20)$$

The expression in (20) contains six integrals, such as  $C_1 - C_6$ . Where,

$$C_1 = \Delta \int_0^\infty t_1 Q_z(g_0 \sqrt{\gamma}, \pi/2) \left\{ \gamma^{\left(mRL + \sum_{i=1}^L n_i\right)^{-1}} - \Theta \gamma^{\left(2mRL + 2 \sum_{i=1}^L n_i\right)^{-1}} \right\} d\gamma . \quad (21)$$

The generalized Marcum  $Q$ -function in (21) is arranged by using the infinite series representation (Simon and Alouini, 2005) as

$$C_1 = \Delta t_1 \exp\left(-\frac{(\pi/2)^2}{2}\right) \sum_{v=1-z}^\infty \left(\frac{g_0}{\pi/2}\right)^v \left(\int_0^\infty \gamma^{\left(mRL + \sum_{i=1}^L n_i\right)^{-1}} \exp\left(-\frac{g_0^2 \gamma}{2}\right) I_v\left(\frac{g_0 \pi}{2} \sqrt{\gamma}\right) d\gamma \right. \\ \left. - \Theta \int_0^\infty \gamma^{\left(2mRL + 2 \sum_{i=1}^L n_i\right)^{-1}} \exp\left(-\frac{g_0^2 \gamma}{2}\right) I_v\left(\frac{g_0 \pi}{2} \sqrt{\gamma}\right) d\gamma \right) \quad (22)$$

Whereby,  $I_v(\dots)$  denotes the modified Bessel function. Representing the modified Bessel function in series as

$$I_v(\lambda) = \left(\frac{1}{2} \lambda\right)^v \sum_{h=0}^\infty \frac{\left(\left(\frac{1}{4}\right) \lambda^2\right)^h}{h! \Gamma(v+h+1)} \quad \text{from (Abramowitz and Stegun, 1970), the above expression becomes}$$

$$C_1 = \Delta t_1 \exp\left(-\frac{(\pi/2)^2}{2}\right) \sum_{v=1-z}^\infty \left(\frac{g_0}{\pi/2}\right)^v \left(\frac{g_0 \pi}{4}\right)^v \sum_{h=0}^\infty \frac{\left(\frac{1}{4}\left(\frac{g_0 \pi}{2}\right)^2\right)^h}{h! \Gamma(v+h+1)} \\ \times \left(\int_0^\infty \gamma^{\left(mRL + \sum_{i=1}^L n_i + v + h\right)^{-1}} \exp\left(-\frac{g_0^2 \gamma}{2}\right) d\gamma - \Theta \int_0^\infty \gamma^{\left(2mRL + 2 \sum_{i=1}^L n_i + v + h\right)^{-1}} \exp\left(-\frac{g_0^2 \gamma}{2}\right) d\gamma \right) \quad (23)$$

Using (Gradshteyn and Ryzhik, 2000), the integrals in (23) can be solved to obtain  $C_1$  as

$$C_1 = \Delta t_1 \exp\left(-\frac{(\pi/2)^2}{2}\right) \sum_{v=1-z}^\infty \left(\frac{g_0^2}{2}\right)^v \sum_{h=0}^\infty \frac{\left(\frac{1}{4}\left(\frac{g_0 \pi}{2}\right)^2\right)^h}{h! \Gamma(v+h+1)} \\ \times \left( \varpi \left(\frac{g_0^2}{2}\right)^{-\left(mRL + \sum_{i=1}^L n_i + v + h\right)} - \Theta \xi \left(\frac{g_0^2}{2}\right)^{-\left(2mRL + 2 \sum_{i=1}^L n_i + v + h\right)} \right) \quad (24)$$

Where,  $\varpi = \Gamma\left(mRL + \sum_{i=1}^L n_i + v + h\right)$  and

$$\xi = \Gamma\left(2mRL + 2 \sum_{i=1}^L n_i + v + h\right)$$

Similarly, by applying the steps involved to obtain  $C_1$ , the expressions of  $C_2 - C_6$  can be obtained as

$$C_2 = \Delta \frac{4}{N} \exp\left(-\frac{(\pi/2)^2}{2}\right) \sum_{v=1-z}^\infty \left(\frac{g_1^2}{2}\right)^v \sum_{h=0}^\infty \frac{\left(\frac{1}{4}\left(\frac{g_1 \pi}{2}\right)^2\right)^h}{h! \Gamma(v+h+1)}$$

$$\times \left( \varpi \left(\frac{g_1^2}{2}\right)^{-\left(mRL + \sum_{i=1}^L n_i + v + h\right)} - \Theta \xi \left(\frac{g_1^2}{2}\right)^{-\left(2mRL + 2 \sum_{i=1}^L n_i + v + h\right)} \right) \quad (25)$$

$$C_3 = \Delta t_2 \exp\left(-\frac{(\pi/4)^2}{2}\right) \sum_{v=1-z}^\infty \left(\frac{g_0^2}{2}\right)^v \sum_{h=0}^\infty \frac{\left(\frac{1}{4}\left(\frac{g_0 \pi}{2}\right)^2\right)^h}{h! \Gamma(v+h+1)}$$

$$\times \left( \varpi \left(\frac{g_0^2}{2}\right)^{-\left(mRL + \sum_{i=1}^L n_i + v + h\right)} - \Theta \xi \left(\frac{g_0^2}{2}\right)^{-\left(2mRL + 2 \sum_{i=1}^L n_i + v + h\right)} \right) \quad (26)$$

$$C_4 = \Delta \frac{8}{N} \sum_{c=1}^{d-1} \exp\left(-\frac{(l_c)^2}{2}\right) \sum_{v=1-z}^\infty \left(\frac{g_0^2}{2}\right)^v \sum_{h=0}^\infty \frac{\left(\frac{1}{4}(g_0 l_c)^2\right)^h}{h! \Gamma(v+h+1)}$$

$$\times \left( \varpi \left(\frac{g_0^2}{2}\right)^{-\left(mRL + \sum_{i=1}^L n_i + v + h\right)} - \Theta \xi \left(\frac{g_0^2}{2}\right)^{-\left(2mRL + 2 \sum_{i=1}^L n_i + v + h\right)} \right) \quad (27)$$

$$C_5 = \Delta \frac{4}{N} \sum_{c=1}^{d-1} \exp\left(-\frac{(s_c^+)^2}{2}\right) \sum_{v=1-z}^{\infty} \left(\frac{g_c^2}{2}\right)^v \sum_{h=0}^{\infty} \frac{\left(\frac{1}{4}(g_c s_c^+)^2\right)^h}{h! \Gamma(v+h+1)} \\ \times \left( \varpi \left(\frac{g_c^2}{2}\right)^{-\left(mRL + \sum_{i=1}^L n_i + v+h\right)} - \Theta \xi \left(\frac{g_c^2}{2}\right)^{-\left(2mRL + 2\sum_{i=1}^L n_i + v+h\right)} \right), \dots\dots\dots(28)$$

and

$$C_6 = \Delta \frac{4}{N} \sum_{c=2}^d \exp\left(-\frac{(s_c^-)^2}{2}\right) \sum_{v=1-z}^{\infty} \left(\frac{g_c^2}{2}\right)^v \sum_{h=0}^{\infty} \frac{\left(\frac{1}{4}(g_c s_c^-)^2\right)^h}{h! \Gamma(v+h+1)} \\ \times \left( \varpi \left(\frac{g_c^2}{2}\right)^{-\left(mRL + \sum_{i=1}^L n_i + v+h\right)} - \Theta \xi \left(\frac{g_c^2}{2}\right)^{-\left(2mRL + 2\sum_{i=1}^L n_i + v+h\right)} \right). \dots\dots\dots(29)$$

**Numerical results**

The derived numerical expressions of OP, ASER with RQAM, as well as ASER with XQAM, have been plotted with arbitrary values of fading parameter ( $m$ ), shadowing parameter ( $p$ ), receiving antennas ( $R$ ) and transmitting antennas ( $L$ ). Figure 3 illustrates the OP comparisons for 2-hop, 4-hop and 9-hop systems with different values of  $p$  and moderate fading ( $m=2.5$ ). In Figure 3,  $L=3$ ,  $R=2$  and  $\gamma_{th} = 1\text{dB}$  are kept constant. It can be seen that OP performance becomes better with  $M=2$  compared to  $M=4$  and  $M=9$ . The probability of an outage increases with the enhancement in the number of hops. The outage performance improves when the system experiences light shadowing ( $p = 10$ ) as compared to moderate shadowing ( $p = 5$ ) and intense shadowing ( $p = 0.5$ ).

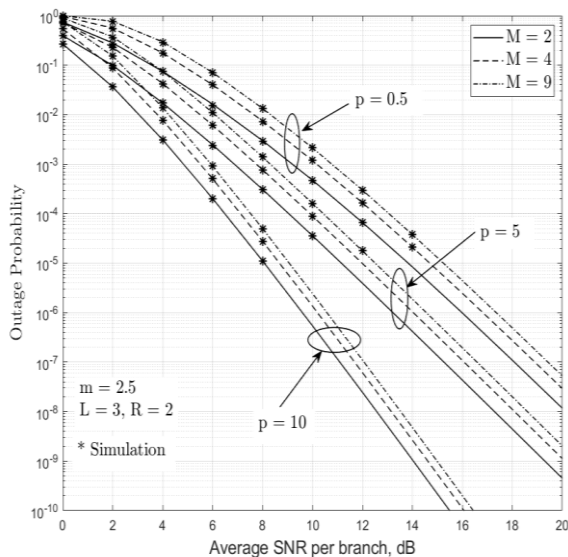


**Figure 3. Outage probability vs. average SNR per branch for different hops employing moderate fading ( $m = 2.5$ ) and different  $p$  values.**

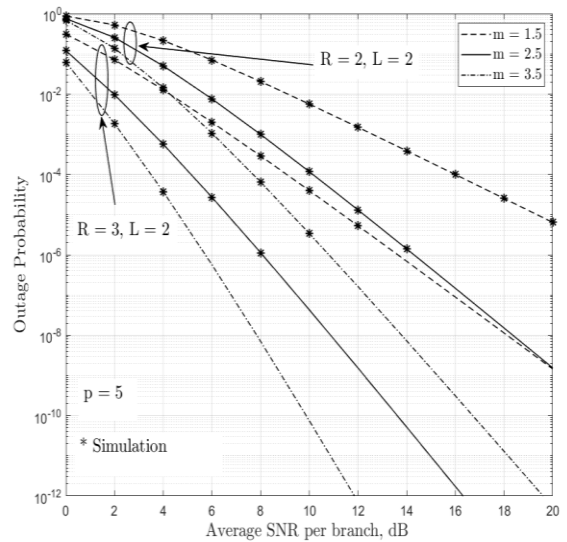


**Figure 4. Outage probability vs average SNR per branch for a 5-hop system for different values of  $R$  and  $m$  with moderate shadowing ( $p = 5$ ).**

Figure 4 plots outage probability performance for the 5-hop link, considering moderate shadowing ( $p=5$ ) and different values of  $m$  and  $R$ . In Figure 4, the value of  $L=2$  is fixed. The system's performance improves with the increment in the values of the  $m$  along with the rise in  $R$ . It is observed that the outage performance improves with  $R=2$  and  $m=3.5$  compared to  $R=3$  and  $m=1.5$  for SNR above 4 dB. An increase in  $m$  makes the system better than increasing the number of  $R$ .

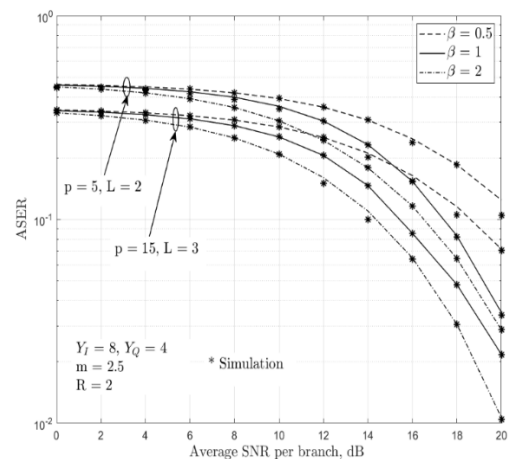


**Figure 5. ASER with  $8 \times 4$  RQAM for different numbers of  $L$ ,  $\beta$  and  $p$  (moderate and light shadowing).**

In Figure 5, the ASER values of the system are illustrated for  $8 \times 4$  RQAM for the 4-hop link with different values of the  $\beta$ ,  $L$  and  $p$ . In Figure 5, the values of  $R=2$  and  $m=2.5$  are considered. The system's performance becomes better when there is light shadowing ( $p = 15$ ) compared to moderate shadowing ( $p = 5$ ), along with the increase in the number of  $L$ . This happens because the power of the direct wave is high

when the values of  $L$  and  $\beta$  increase. So, it results in a better channel.

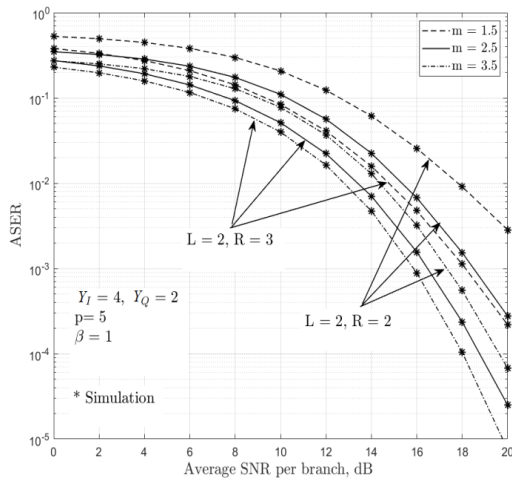


**Figure 6.** ASER with  $4 \times 2$  RQAM for different values of  $R$  and  $m$  considering moderate shadowing ( $p = 5$ ) and  $\beta=1$ .

In Figure 6, the ASER performance of  $4 \times 2$  RQAM is depicted for 6-hop link with moderate shadowing ( $p=5$ ) and  $\beta = 1$  employing different values of  $m$  and  $R$ . System performance becomes better when there is an increase in  $m$  and  $R$ . This happens because the probability of deep fading decreases for the more redundant path.

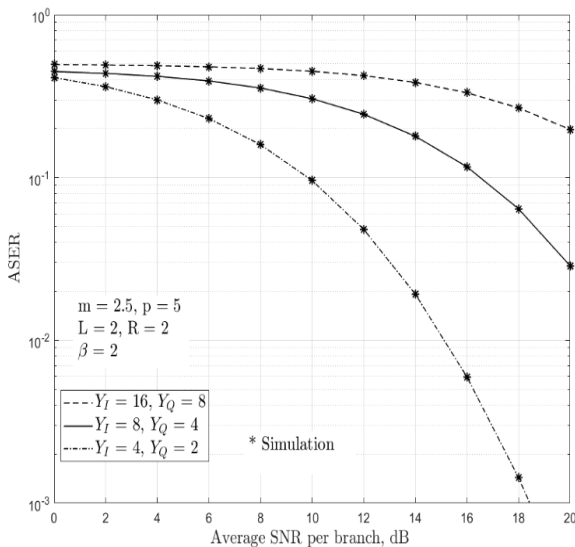


**Figure 7.** ASER comparison results of RQAM with different constellation sizes and the 5-hop system.

In Figure 7, the ASER comparison of RQAM with different constellation sizes and for 5-hop link are plotted with  $\beta = 2$ ,  $m = 2.5$ ,  $p = 5$ ,  $L = 2$ , and  $R = 2$ . It is realized that the ASER performance of  $4 \times 2$  RQAM is superior as compared to  $8 \times 4$  RQAM as well as  $16 \times 8$  RQAM, since the SNR gain is greater for smaller values of the constellation size, and it gradually decreases with the increase in constellation size.

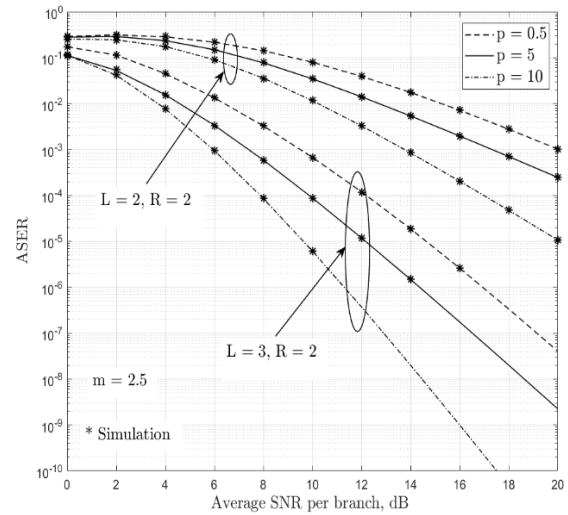


**Figure 8.** ASER with 32-XQAM for different  $p$  and  $L$  considering 5-hop system and moderate fading ( $m = 2.5$ ).

Figure 8 plots the ASER performance for 32-XQAM with 5-hop using different  $p$  and  $L$  values. In Figure 8,  $m=2.5$  is a fixed value. The system's performance becomes better with the increment in  $p$ , i.e. when the system experiences light shadowing along with the increase in  $L$ .

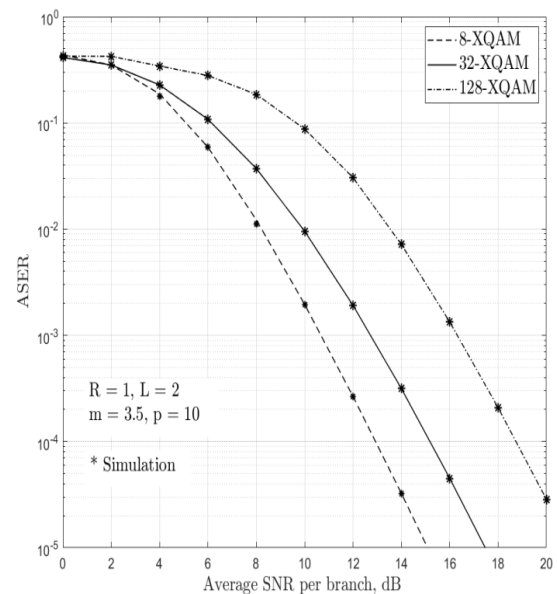


**Figure 9.** Comparison results of different XQAM for 6-hop system.

In Figure 9, the ASER comparison of different XQAM for the 6-hop systems are illustrated with different values of  $N$  considering  $m = 3.5$ ,  $p = 10$ ,  $R = 1$  and  $L = 2$ . The performance of 8-XQAM dominates compared to 32-XQAM and 128-XQAM because the SNR gain is high for smaller values of  $N$ .



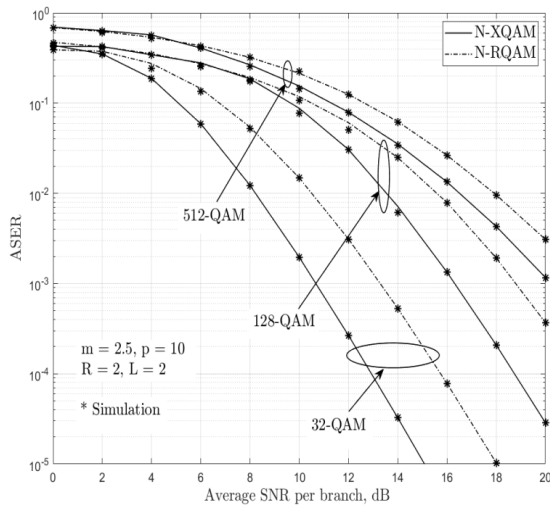


**Figure 10. ASER comparison results of  $N$ -XQAM and  $N$ -RQAM.**

Figure 10 illustrates the comparison results of different  $N$ -XQAM and  $N$ -RQAM for the 4-hop system. In Figure 10,  $m = 2.5$ ,  $p = 10$ ,  $L = 2$  and  $R = 2$  are considered. It is noticed that XQAM displays SNR gain compared to RQAM.

### Conclusion

This work thoroughly investigates the TAS/MRC-based MIMO multihop communication system, which operates under Fisher-Snedecor  $F$  fading channels. It primarily examined the Average Symbol Error Rate (ASER) using Rectangular Quadrature Amplitude Modulation (RQAM) and Cross QAM (XQAM) approaches. The results were thoroughly confirmed using Monte-Carlo simulations. The analytical findings correlate strongly with the computationally produced data and have been visually depicted for enhanced clarity. We analyzed the effects of Fisher-Snedecor  $F$  fading on the system by examining several values of parameters, including  $m$ ,  $p$ ,  $L$ ,  $R$ , and  $\beta$ . We also considered an unlimited number of hops. The system's performance improvement is notably affected by both  $m$  and  $p$ , demonstrating the combined impact of shadowing and multipath fading. In addition, we investigated the chance of the system experiencing an outage (OP) and the average symbol error rate (ASER). Our analysis specifically concentrated on decode-and-forward relaying in a communication scenario including many hops. Analyzed was the suggested MIMO system employing Transmit Antenna Selection/Maximal Ratio Combining (TAS/MRC), which shows that increasing the number of hops leads to an augmentation in OP. Increased variation in the number of hops leads to enhanced overall system performance.

Additionally, our analysis uncovered that the fading parameter notably influences the system's performance, wherein lighter shadowing circumstances result in enhanced ASER (Average Symbol Error Rate) and OP (Outage Probability). In addition, we conducted a performance comparison between RQAM and XQAM, emphasizing the superiority of XQAM in terms of Signal-to-Noise Ratio (SNR) improvement over RQAM. Increasing the number of antennas might lead to higher costs, and providing accurate input to the transmitting node is essential for selecting the most effective antennas. Overall, the study of the TAS/MRC-based MIMO multihop communication system, examined in the context of Fisher-Snedecor  $F$  fading channels, shows encouraging enhancements in performance. This is particularly evident when considering factors such as  $m$ ,  $p$ , fading conditions, and the number of hops. The findings obtained from this study enhance comprehension of the system's behaviour and offer useful direction for enhancing the design and implementation of similar communication systems.

### Conflict of Interest

The authors declare no conflict of interest.

### References

- Abramowitz, M., & Stegun, I. A. (1970). Handbook of Mathematical Functions, With, Graphs, and Mathematical Tables. Dover Publications, Inc., USA.
- Agarwal, D. P., & Zeng, Q. A. (2011). *Introduction to Wireless and Mobile Systems*, 2<sup>nd</sup> edition, Hoboken, New Jersey, USA: Wiley.
- Al-Hmood, H., & Al-Raweshidy, H. S. (2021). Selection combining scheme over non-identically distributed Fisher-Snedecor  $F$  fading channel. *IEEE Wireless Communications Letters*, 10(4), 840-843. <https://doi.org/10.1109/LWC.2020.3046519>
- Badarneh, O. S., da Costa, D. B., Sofotasios, P. C., Muhaidat, S., & Cotton, S. L. (2018). On the sum of Fisher-Snedecor  $F$  variates and its application to maximal ratio combining. *IEEE Wireless Communications Letters*, 7(6), 966-969. <https://doi.org/10.1109/LWC.2018.2836453>
- Banu, D. F., Pradeep, R., Hakeem, B., & Kayathri, T. L. (2022). Performance improvement in cooperative communication wireless network using QAM decode-and-forward protocol. *8<sup>th</sup> International Conference on Advanced Computing and Communication Systems (ICACCS)*, Coimbatore, 1996-2000.

- <https://doi.org/10.1109/ICACCS54159.2022.9784994>
- Bao, V. N. Q., & Kong, H. Y. (2010). Performance analysis of decode and forward relaying with partial relay selection for multi-hop transmission over Rayleigh fading channels. *Journal of Communications and Networks*, 12(5), 433-441. <https://doi.org/10.1109/JCN.2010.6388488>
- Beaulieu, N. C. (2006). A useful integral for wireless communication theory and its application to rectangular signalling constellation error rates. *IEEE Transactions on Communications*, 54(5), 802–805. <https://doi.org/10.1109/TCOMM.2006.874003>
- Chiani, M., Dardari, D., & Simon, M. K. (2003). New exponential bounds and approximations for the computation of error probability in fading channels. *IEEE Transactions on Wireless Communication*, 2(4), 840-845. <https://doi.org/10.1109/TWC.2003.814350>
- Clarke, P., & De Lamare, R. C. (2012). Time diversity and relay selection algorithms for multi-relay cooperative MIMO systems. *IEEE Transactions on Vehicular Technology*, 61(3), 1084-1098. <https://doi.org/10.1109/TVT.2012.2186619>
- Dixit, D., & Sahu, P. R. (2013). Performance of QAM signalling over TWDP fading channels. *IEEE Transactions on Wireless Communication*, 12(4), 1794-1799. <https://doi.org/10.1109/TWC.2013.030413.120772>
- Dixit, D., & Sahu, P. R. (2018). Performance of multihop detect-and-forward relaying system over fluctuating two-ray fading channel. *Transactions on Emerging Telecommunications Technologies*, 29(8). <https://doi.org/10.1002/ett.3423>
- Foschini, G. J., & Gans, M. J. (1998). On the limits of wireless communications in a fading environment when using multiple antennas. *Wireless Personal Communications*, 6(3), 311-335. <https://doi.org/10.1023/A:1008889222784>
- Gradshteyn, I. S., & Ryzhik, I. M. (2000). Table of integrals, Series and Products. 6<sup>th</sup> edition, San Diego, CA: Academic.
- Ikki, S. S., & Ahmed, M. H. (2010). On the performance of cooperative diversity network with  $N^{th}$  best-relay selection scheme. *IEEE Transaction Communications*, 58(11), 3062-3069. <https://doi.org/10.1109/TCOMM.2010.092810.090322>
- Ikki, S. S., & Aissa, S. (2012). Multihop wireless relaying system in presence of cochannel interferences: Performance analysis and design optimization. *IEEE Transactions on Vehicular Technology*, 61(2), 566-573. <https://doi.org/10.1109/TVT.2011.2179818>
- Kumbhani, B., & Kshetrimayum, R. S. (2016). Performance analysis of MIMO systems with antenna selection over Generalized  $\kappa$ - $\mu$  fading channels. *IETE Journal of Research*, 62(1), 45-54. <https://doi.org/10.1080/03772063.2015.1082444>
- Laneman, J. N., Tse, D. N., & Wornell, G. W. (2004). Cooperative diversity in wireless networks: Efficient protocols and outage behaviour. *IEEE Transactions on Information Theory*, 50(12), 3062-3080. <https://doi.org/10.1109/TIT.2004.838089>
- Molisch, A. F., & Win, Z. M. (2004). MIMO systems with antenna selection. *IEEE Microwave Magazine*, 5(1), 46-56. <https://doi.org/10.1109/MMW.2004.1284943>
- Nosratinia, A., Hunter, T.E., & Hedayat, A. (2004). Cooperative communication in wireless network. *IEEE Communications Magazine*, 42(10), 74-80. <https://doi.org/10.1109/MCOM.2004.1341264>
- Oyman, O., Laneman, J. N., & Sandhu, S. (2007). Multi-hop relaying for broadband wireless mesh networks: From theory to practice. *IEEE Communication Magazine*, 42(11), 116-122. <https://doi.org/10.1109/MCOM.2007.4378330>
- Pabst, R., Walke, B. H., Schultz, D. C., Herhold, P., Yanikomeroğlu, H., Mukherjee, S., Viswanatham, H., Lott, M., Zirwas, W., Dohler, M., Aghvami, H., Falconer, D. D., & Fettweis, G. P. (2004). Relay-based deployment concepts for wireless and mobile broadband radio. *IEEE Communication Magazine*, 42(9), 80-89. <https://doi.org/10.1109/MCOM.2004.1336724>
- Rappaport, T. S. (2011). *Wireless Communication*, 2<sup>nd</sup> edition, Chennai, India: Pearson.
- Proakis, J. G. (2001). *Digital Communications*, 4<sup>th</sup> edition, New York, NY, USA: McGraw Hill.
- Sanayei, S., & Nosratinia, N. (2004). Antenna selection in MIMO systems. *IEEE Communication Magazine*, 42(10), 68-73. <https://doi.org/10.1109/MCOM.2004.1341263>
- Sendonaris, A., Erkip, E., & Aazhang, B. (2003). User cooperation diversity - part I. System description. *IEEE Transactions on Communications*, 51(11), 1927-1938. <https://doi.org/10.1109/TCOMM.2003.818096>
- Shaik, P., Singya, P. K., & Bhatia, V. (2019). On impact of imperfect CSI over Hexagonal QAM for TAS/MRC MIMO cooperative relay network.

- IEEE Communication Letters*, 23(10), 1721-1724.  
<https://doi.org/10.1109/LCOMM.2019.2931433>
- Simon, M. K., & Alouini, M. S. (2005). *Digital communication over fading channels*, 2<sup>nd</sup> edition, John Wiley & Sons.
- Singya, P. K., Kumar, N., Bhatia, V., & Khan, F. A. (2018). Performance analysis of OFDM based 3-hop AF relaying network over mixed Rician/Rayleigh fading channels. *AEU-International Journal of Electronics and Communication*, 93, 337-347.  
<https://doi.org/10.1016/j.aeue.2018.06.026>
- Smith, J. G. (1975). Odd-bit quadrature amplitude-shift keying. *IEEE Transaction Communication*, 23(3), 385-389.  
<https://doi.org/10.1109/TCOM.1975.1092806>
- Stuber, G. L. (2003). *Principles of Mobile Communication*, 2<sup>nd</sup> edition, Norwell, MA, USA: Kluwer.
- Yoo, S. K., Cotton, S. L., Sofotasios, P. C., Matthaiou, M., Valkama, M. & Karagiannidis, G. K. (2017). The Fisher-Snedecor  $F$  distribution: A simple and accurate composite fading model. *IEEE Communication Letters*, 21(7), 1661-1664.  
<https://doi.org/10.1109/LCOMM.2017.2687438>
- Yu, H., Wei, G., Ji, F., & Zhang, X. (2011). On the error probability of cross-QAM with MRC reception over generalized  $\eta$ - $\mu$  fading channels. *IEEE Transactions on Vehicular Technology*, 60(6), 2631-2643.  
<https://doi.org/10.1109/TVT.2011.2154347>
- Zhang, X.-C., Yu, H., & Wei, G. (2010). Exact symbol error probability of cross-QAM in AWGN and fading channels. *EURASIP Journal on Wireless Communications and Networking*, 2010, 1-9.  
<https://doi.org/10.1155/2010/917954>

#### How to cite this Article:

Hubha Saikia and Rajkishur Mudoi (2023). Analyzing the Performance of TAS/MRC with Decode-and-Forward Relaying for Multihop Transmission over Fisher-Snedecor  $F$  Fading Channels. *International Journal of Experimental Research and Review*, 36, 116-126.

DOI : <https://doi.org/10.52756/ijerr.2023.v36.011>



This work is licensed under a Creative Commons Attribution-NonCommercial-NoDerivatives 4.0 International License.